IR sensor performance testing with a double-slit method

Arie N. de Jong, Hans Winkel, Rick Ghauharali

TNO Physics and Electronics Laboratory
PO Box 96864, 2509 JG The Hague, The Netherlands
E-mail: dejong@fel.tno.nl

ABSTRACT

Determination of the performance of undersampled IR cameras by means of four-bar patterns suffers from aliasing for spatial frequencies above the Nyquist limit. An alternative method, using two parallel line sources, is described. This method avoids the aliasing effect and allows a reproduceable way for performance measurements by simple variation of the spacing between the two line sources and their temperatures. The modulation depth at optimum phase is measured in the camera display or electronics, similar to the classical Rayleigh criterion. Additional benefits of the new method are the simple target construction (only one target is required) and the ease to model line sources. The result of a performance measurement is similar to the standard MRTD (Minimum Resolvable Temperature Difference) method, where sensor resolution is coupled to range for a given target size and contrast. The new method has therefore the potential to be implemented into the present STANAG4347 and 4349. Results of performance measurements, carried out with the uncooled Thermacam PM395 camera and other cameras, are shown. Predicted and measured performance agree very well.

1. INTRODUCTION

Aliasing is a well-known optical phenomenon, occurring when regular bar patterns are imaged with a camera with discrete sampling or fixed detector positions at similar spatial frequencies as the observed bar pattern. For observers this means that the perceived modulation depth depends on the position of the sampling grid with respect to the bars (phase in space) and can become zero when the bar period is twice the sample distance or detector pitch. The corresponding spatial frequency is called the Nyquist frequency. For higher spatial frequencies it is impossible to count the proper number of bars, although there is still a perceivable modulation. This modulation appears to run quickly in the direction of movement, when the phase between bar pattern and sampling grid is changed.

In standard MRTD measurements on undersampled imagers, the MRTD curve stops at the Nyquist frequency. Wittenstein has developed the MTDP (Minimum Temperature Difference Perceived) approach [1], using the remaining modulation depths at frequencies above the Nyquist limit. This principle is applied in the German Thermal Range Model TRM3 [2]. In this model the AMOP (Average Modulation at Optimum Phase) is measured. A problem is that the AMOP can not be predicted analytically. Furthermore the problem remains of the loss in proper counting of the number of bars, which is essential in the MRTD measurement method, described in STANAG4349 [3].

One solution to the problem of number counting is to work with the concept of objective MRTD by using a tilted line source and selecting the optimum LSF (Line Spread Function). This method was developed at TNO-FEL [4] and applied in an Infrared zoom collimator [5]. In a comparative test a large number of IR cameras were tested. More recently one test unit was built for the Ophelios camera, where the image is taken at the video output and one tester was built for the LION handheld camera, where the image is taken from the eye piece [6]. The advantage of the objective MRTD method is its reproduceability and the cost savings when series of similar cameras are tested.

In order to include a human observer in IR camera performance test procedures, it is a logical step to take two line sources instead of one and put forward as perception task the ability to see the two lines separated similar to the classical approach of Rayleigh in discriminating two point sources [7]. The principle task is then to find the minimum angular separation of two parallel line sources that can just be discriminated as function of their signal to noise ratio. A major advantage of the use of the LSF (and two LSF's) is the ease to model them and their direct relationship with the MTF (Modulation Transfer Function) and the MRTD by their Fourier Transform. This is a problem in other alternative targets such as the Landolt-C rings in acuity test for the eye or the triangles, as proposed by TNO-TM [8]. In field tests of airborne reconnaissance cameras, there may be a benefit of using two non-parallel line sources, allowing full resolution analysis from just a few frames. This method has been successfully used with the RISTA II sensor of Northrop Grumman for the F16 and the SPERWER-IRIS camera of SAGEM for the Army UAV.

Infrared Imaging Systems: Design, Analysis, Modeling, and Testing XII, Gerald C. Holst, Editor,
Proceedings of SPIE Vol. 4372 (2001) © 2001 SPIE · 0277-786X/01/$15.00

2. BACKGROUND CONSIDERATIONS

The use of 4-bar patterns in IR sensor performance testing is attractive as the target represents approximately one spatial frequency, allowing easy operation in the Fourier domain together with MTF's of sensor components [9]. On the other hand the 4-bars have little resemblance with real IR target signatures. In addition, staring IR cameras demonstrate a high sensitivity with NETD (Noise Equivalent Temperature Difference) values of less than 25 mK and in the future possibly less than 5 mK.
This implies big problems in the classical MRTD setup where a temperature stability and accuracy of 1 mK is required. In effect, a proper MRTD measurement at low spatial frequencies is only possible when using an IR neutral density filter with 10× attenuation.
The undersampling effect, mentioned in the introduction, and already present in the vertical direction in classical 1st generation scanning IR cameras, appears dominant at high spatial frequencies in the 3rd generation staring cameras in both horizontal and vertical direction. A more detailed consideration is illustrated by means of Figure 1, where a and b are the dimensions of the sensitive area of one detector in vertical respectively horizontal direction, a_p and b_p the pitch in these directions and d_s and d_b the separation between two parallel line sources respectively one period of the bar pattern as projected in the focal plane.

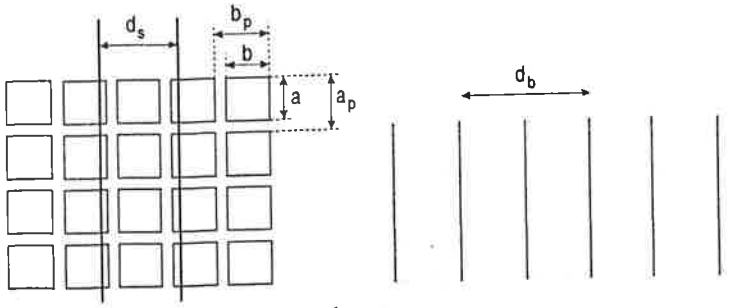

Figure 1: Double-slit and bar pattern on 2-dimensional array of detectors.

Aliasing with the bar pattern starts to occur when $\frac{1}{2} d_b$ approaches b_p; when $\frac{1}{2b_p}$ equals $\frac{1}{d_b}$, we are at the Nyquist frequency.

Signal modulations are only found if the phase is correct. When b_p equals d_b, no modulation is found for whatever phase is taken. For $b_p > d_b$, modulations can principally return.
For the line sources (or double-slit), modulation disappears however when the separation distance d_s equals b_p and does not reappear for cases that $b_p > d_s$. For $b_p < d_s$, the optimum phase has to be found providing the highest modulation for the center row of detectors compared to the neighboring rows.

If we consider in some more detail the imaging aspects of the two line sources, the two intensity distributions $I_1(x)$ and $I_2(x)$, produced by the IR camera objective lens in the focal plane, partly overlap, as shown in Figure 2. When the separation distance d_s is becoming smaller, the modulation depth M, defined as the ratio of the intensity dip I_d in the middle and the peak intensity I_p, becomes smaller.

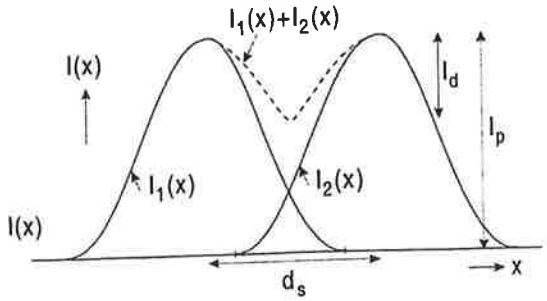

Figure 2: Intensity distribution of double-slit in focal plane.

Striking is the strong dependence of the modulation depth on the slit separation distance. If for example for $I_1(x)$ and $I_2(x)$ Gaussian functions are taken:

$$I_1(x) = I_2(x) = e^{-2\frac{x}{\sigma^2}} \tag{1}$$

the resulting curves of M versus d_s are shown for σ values of 2 and 4. If we put a discrimination threshold at M = 0.1, the corresponding d_s values are 2.5 and 5. An increase of a few percent in the value of d_s provides a strong increase (factor 2) in M. The interaction of the intensity distribution $I_1(x) + I_2(x)$ with the sampling by the detectors is further discussed in the next chapter. Interesting is to notify the behaviour of the phenomena in the Fourier domain. The Fourier transform ([10]) of two line sources (infinitesimal narrow) becomes:

$$F(f) = \int_{-\infty}^{\infty} \left\{ \delta\left(x + \frac{d_s}{2} \right) + \delta\left(x - \frac{d_s}{2} \right) \right\} e^{-2\pi j f x} dx = 2\cos \pi f d_s \tag{2}$$

This function becomes zero for $f = \frac{1}{2d_s}$; comparing to one line source, having a white spectrum, or to a 4-bar pattern, having approximately a dedicated spatial frequency, the double line source is a kind of intermediate between the two other types of targets.

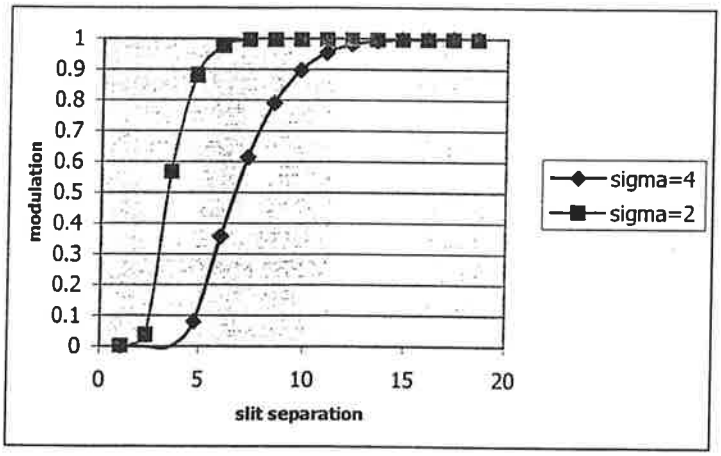

Figure 3: Modulation depth M versus distance d_s between 2 line sources with Gaussian blur.

An essential issue is to make a link to observer perception performance, based upon double-slit separation. Comparable to Johnsons criteria, which state that for 50% recognition probability 3 line pairs per minimum target dimension are required, we can introduce a type of MRTD curve for a double line source MRID. This curve provides the Minimum Radiant Intensity Difference per unit line length required to perceive the double line source just separated, as function of the inverse separation distance $\frac{1}{d_s}$ (Figure 4).

The number N of spatial details at distance d_s per target size d_t required for 50% recognition probability is likely to be close to 3 because of the 3 line pairs, taken in the STANAG, following the Johnsons criteria [9]. The number of 3 has however to be validated by means of perception experiments. The recognition range R_{rec} follows immediately from:

$$R_{rec} = \frac{d_t}{N} \cdot \frac{1}{d_s} \tag{3}$$

where d_s stands for the vision limited separation distance for a given Radiant Intensity Contrast. It is noted that observers make a decision on the visibility of two separated lines and that the problem of running 2 or 3 bars instead of the presented 4 bars does not occur in this case.

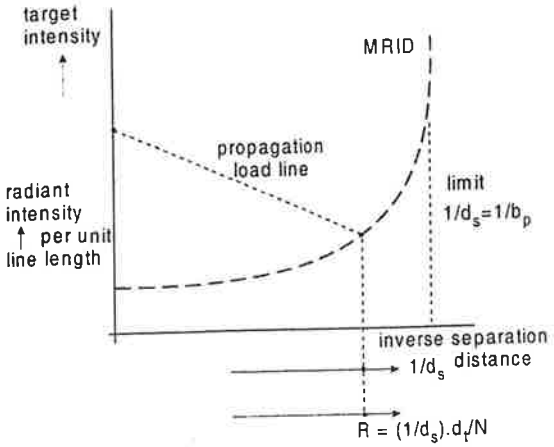

Figure 4: MRID curve and its use for range determination similar to STANAG4347.

3. MODELLING

Modelling of the image transfer of a double line source through an IR imaging camera is rather straightforward. A numerical model has been developed, predicting the camera response (output) for a selection of input parameters, listed in Table 1.

Table 1: Input parameters for double-slit model

double-slit parameters	camera parameters
slit-to-camera distance	focal length
slit-slit separation distance	equivalent optics blur
slit width	pixel size, fill factor
slit-background contrast	phase between slits and FPA grid
	equivalent noise amplitude
	electronics time constant

The simple model, running in Microsoft Excel, calculates the total blur, assumed as a Gaussian curve with width w_t as a kind of sum of diffraction blur $w_d = 1.22\lambda f_\#$, slit width w_o and aberration blur w_b by means of the formula

$$w_t = \sqrt{w_d^2 + w_o^2 + w_b^2} \tag{4}$$

where λ is the wavelength and $f_\#$ the f-number of the optics. If this Gaussian intensity distribution is projected onto an FPA (Focal Plane Array) detector, the sampling of a single slit may be as shown in Figure 5.

Three neighboring elements (1), (2) and (3) respond to the projected image. The video output is calculated from the electronics impulse response function p(t):

$$\left.\begin{aligned} p(t) &\propto \{1-\exp(-t/\tau)\} && t<\Delta t \\ &\propto \{1-\exp(-\Delta t/\tau)\}\cdot\exp\{-(t-\Delta\tau)/\tau\} && t\geq\Delta t \end{aligned}\right\} \tag{5}$$

in which τ is the electronics response time and Δt the pulse width.
The response graphs for a double-slit target is shown in Figure 6, where input parameters were used from the uncooled Thermacam PM395 camera with 13° lens and a realistic target setup with 2 heated wires at 21 m distance. The model is very illustrative in showing the phase effects and is of great help in studies on the influence of sensor parameters on resolution. The model is rather quick; the calculations for Figure 6 were done in 1 second.

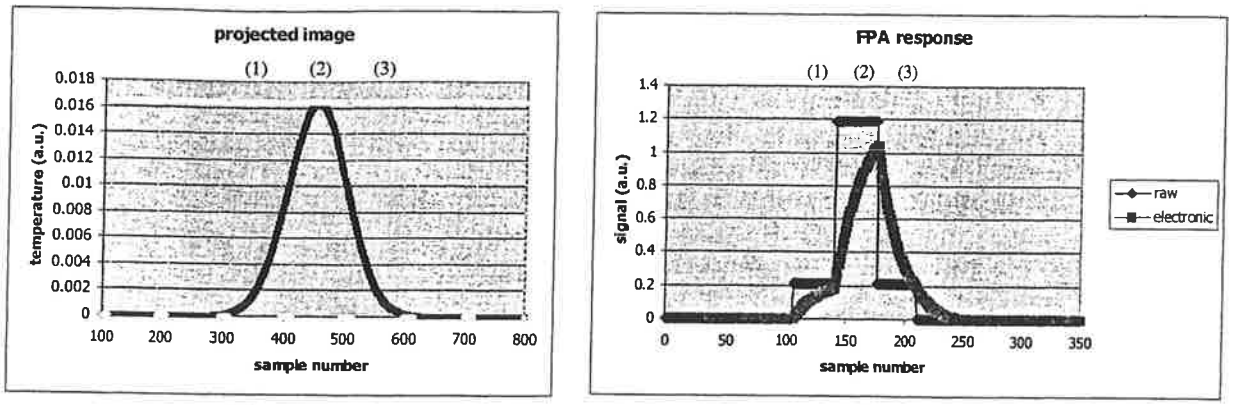

(a) (b)

Figure 5: Sampling of Gaussian intensity plot by FPA grid (a) and response in the CCD (black) and after the electronics.

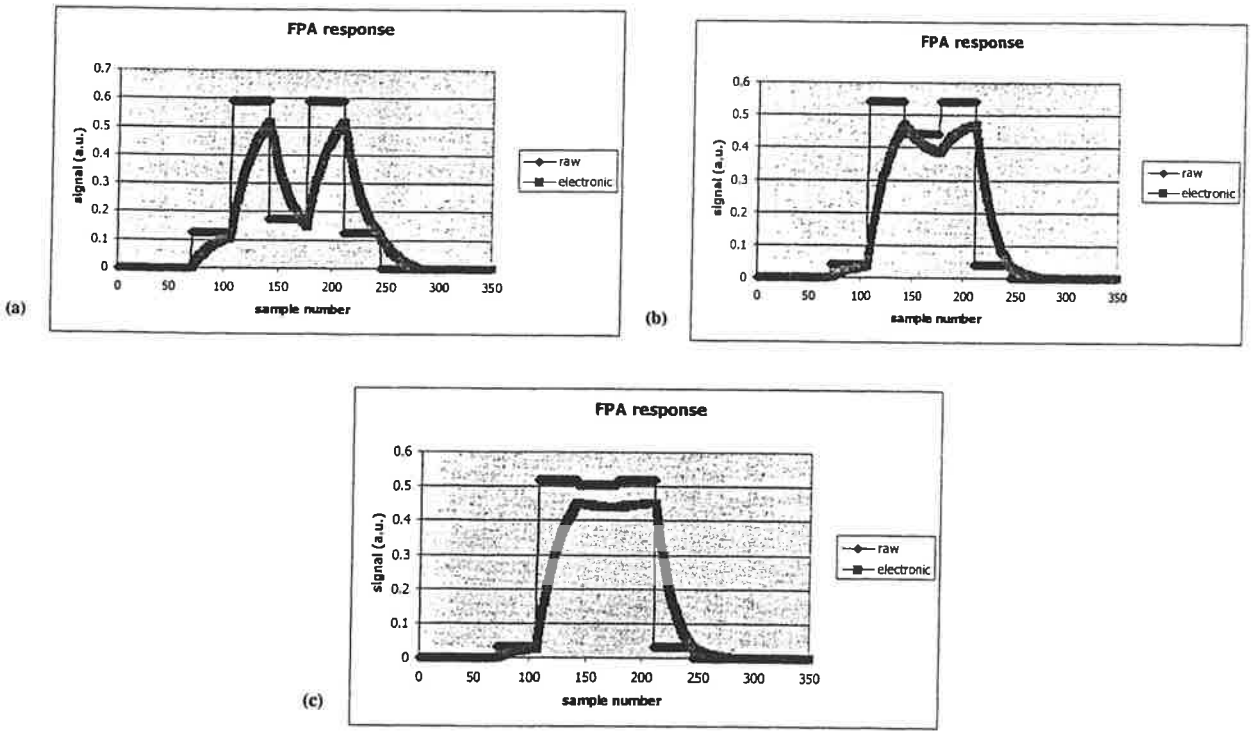

Figure 6: Response graphs for double-slit patterns. (a) – (c) decreasing slit-slit separation.

A similar routine was developed in Matlab, allowing to show real imagery. An example is given in Figure 7.

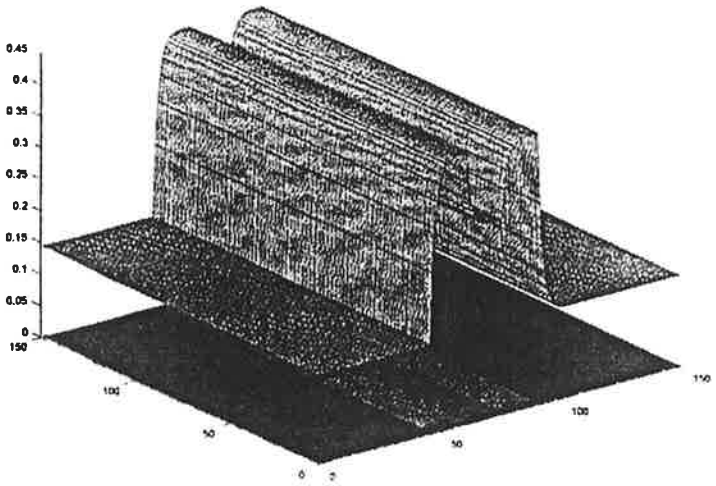

Figure 7: Output from Matlab simulation.

4. MEASUREMENT RESULTS

It was decided to start the experiments with double line sources on a larger scale in the dark tunnel at TNO-FEL. A setup was built as shown in Figure 8: a single heating wire up and down, kept in straight lines by means of springs in the bottom. The distance between the wires could be varied between 18 and 120 mm. The heating wire had a diameter of 0.75 mm and a specific resistance of 3.28 Ω/m. The length of the wires was 260 mm, about 14× the minimum distance.

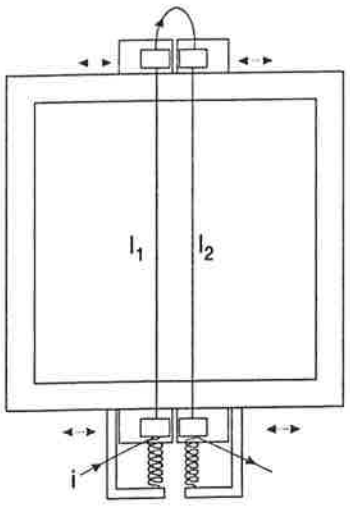

Figure 8: Sketch of double line source setup for experiments in dark tunnel at TNO-FEL.

A list of the cameras, that have been tested with the double-slit method, is given in Table 2.

Table 2: List of cameras, used in double slit experiments.

Type	Company	Spectral band	No of detectors	FOV	Detector pitch	Remarks
Thermacam PM395	Inframetrics	7.6-13.5 μm	320×240	13°×10°	0.71 mr	Uncooled VOX
Thermacam PM395	Inframetrics	7.6-13.5	320×240	26°×20°	1.42	Uncooled VOX
Thermacam PM200	Inframetrics	3.35-4.20	256×256	8°×8°	0.55	PtSi
Radiance I	Amber	3-5	256×256	5.6°×5.6°	0.38	InSb
IR18	Barr & Stroud	7.2-10.8	4×6	6°×4°	0.3	Scan/Sprite

Three of the cameras were equipped with a Focal Plane Array, one was a classical scanning camera.
For all the cameras the following characteristics were measured:

- responsivity at a given gain setting and ambient temperature (20°C)
- NETD (Noise Equivalent Temperature Difference) per pixel, per frame and in one videoline
- LSF at various phases of the line on the detector grid
- modulation depth as function of line separation distance d_s.

For the sake of simplicity only vertical bars and lines were measured. For the PM395 camera, two lenses were available, one with wide field of view (26° horizontal) and one with half of that field of view. A summary of the data is given in Table 3, including the limiting separation distance $d_s(l)$ at 10% modulation depth level. Examples of imagery of 4-bars and double-slits are shown in Figure 9. The figure shows clearly the aliasing effect in the undersampled Thermacam 395 (with 13° FOV lens) when imaging the 4-bar pattern. From Table 2 it is noted that the detector pitch (sampling distance) of 0.71 mr corresponds to a Nyquist frequency of 0.70 c/mr, so the higher frequencies appear with the wrong bar number. The imagery on the right of double slits shows the phase effect with tilted slits and a just discernable double-slit with a slit separation distance of 0.92 mr.

Table 3: Summary of sensor performance data.

Camera	FOV	Responsivity	Span/Gain	NETD			$d_s(l)$ 10%
				picture	pixel	line	
Thermacam PM395 (13°)	13°×10°	160 mV/°C	3.4	0.094°	0.084°C	0.098°C	0.88 mr
Thermacam PM395 (26°)	26°×20°	190	3.0	0.084	0.067	0.098	1.70
Thermacam PM200	8°×8°	220	2.8	0.069	0.060	0.090	0.65
Radiance I	5.6°×5.6°	165	4.49	0.037	0.031	0.043	0.45
IR18	6°×4°	150	2	0.30	0.25	0.37	0.34

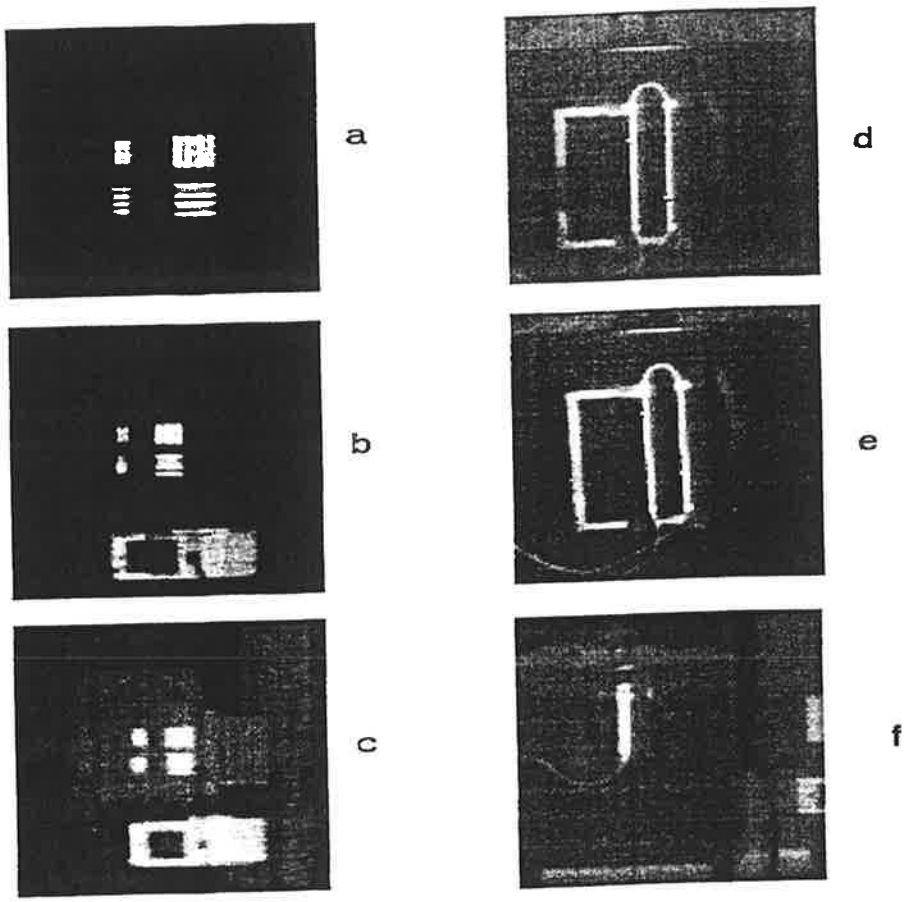

Figure 9: Imagery taken with uncooled Thermacam PM395 with 13° lens

a,b,c	4 bar pattern
d,e,f	double slits
a:	bar spatial frequency 0.56 c/mr showing 4 bars
b:	0.86 c/mr showing 3 bars
c:	0.98 c/mr showing 2 bars; $f_{Nyquist} = 0.70$ c/mr
d:	slit distance 7.7 mr
e:	tilted slits showing phase effect
f:	slit distance 0.92 mr; slits just discernable

Figure 10 shows samples of video signals for both types of targets at various spatial frequencies. The signal plots on the left could directly be used to determine the AMOP for the MTDP. The signal plots on the right were used to determine the modulation depth M. The results for all 5 cameras of Tables 2 and 3 are plotted in Figure 11, showing the steep slopes of the M curves against slit spacing, corresponding to the curves of Figure 3.
The double slit method apparently does not only work for undersampled (FPA) imagers, but of course is also working quite well for well sampled sensors such as the IR18. The only difference is that for the well sampled cameras it is not necessary to search for the optimum phase.
The measurements of the MTF, AMOP and modulation depths were used to determine the range, at which a NATO standard target of 2.3×2.3 m can be recognized for the classical MRTD method, limited by aliasing, the MTDP following the TRM3 model and the MRID with the two line sources. The result is shown in Figure 12. The classical range R_1 is too pessimistic. The MTDP continues beyond the Nyquist frequency f_N and the MRID, assuming a number N of details of 3 is providing the longest recognition range. The main reason is the fact that the peak modulation with 2 slits is in principle higher than the average modulation following the AMOP method for 4 bars with the same period. Values R_1, R_2 and R_3 are respectively

540 m, 810 m and 880 m. The value of 880 m corresponds better to the ranges, found in a preliminary field experiment, carried out by NATO group TG16 in Nettuno (Italy) with the PWTIC uncooled camera from Texas Instruments with performance data similar to the PM395 [11]. Further field experiments will be required to see how realistic these predictions from laboratory measurements are.

In view of the importance of feature details in the identification process, especially when the probability level of identification is increased from 50% to say 90%, it is highly probable that detail discrimination will dominate.

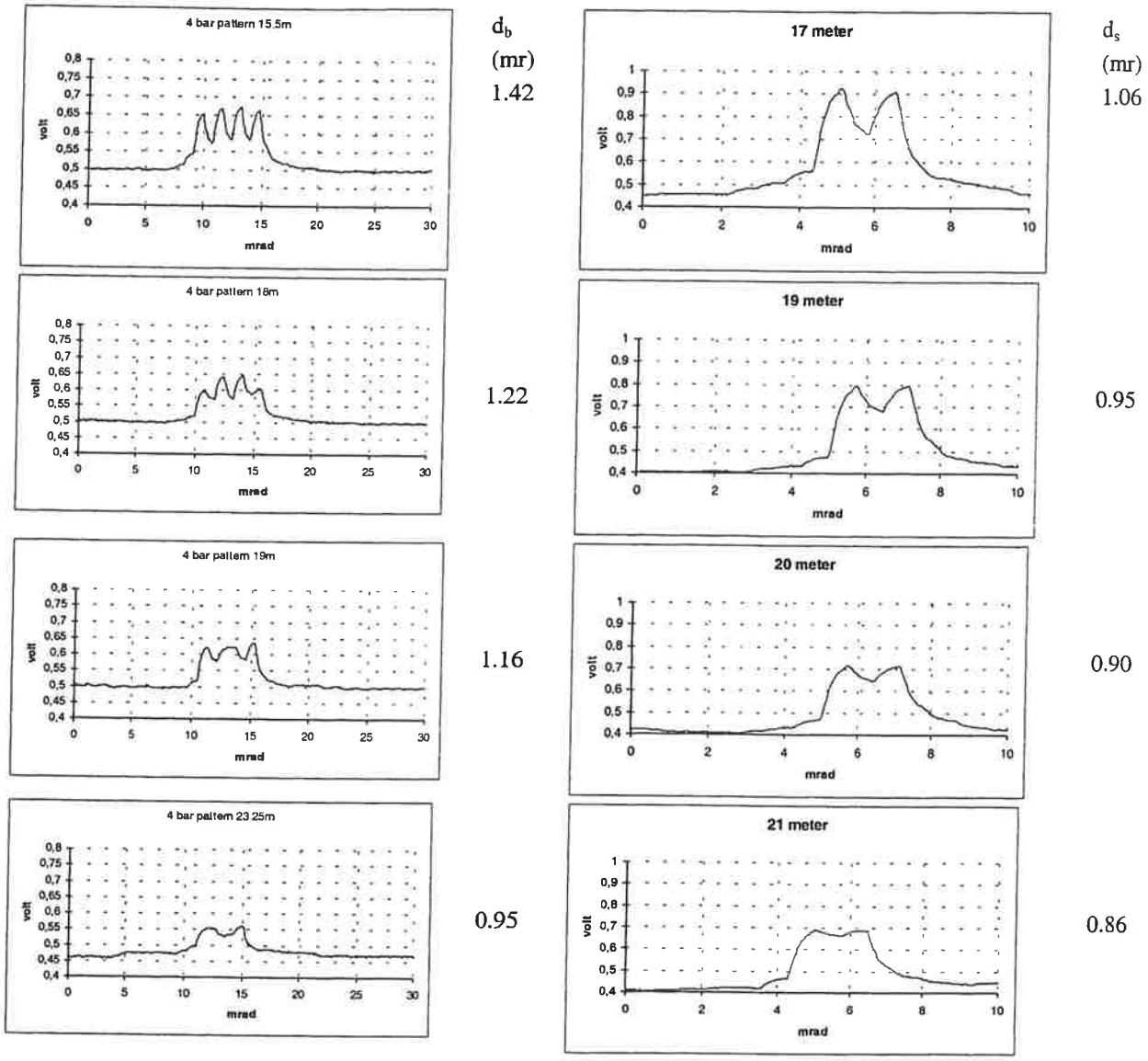

Figure 10: Video responses from Thermacam PM395 with 13° lens on 4-bar patterns and double line sources at given distances; Bar period 22 mm; Line separation distance 18 mm.

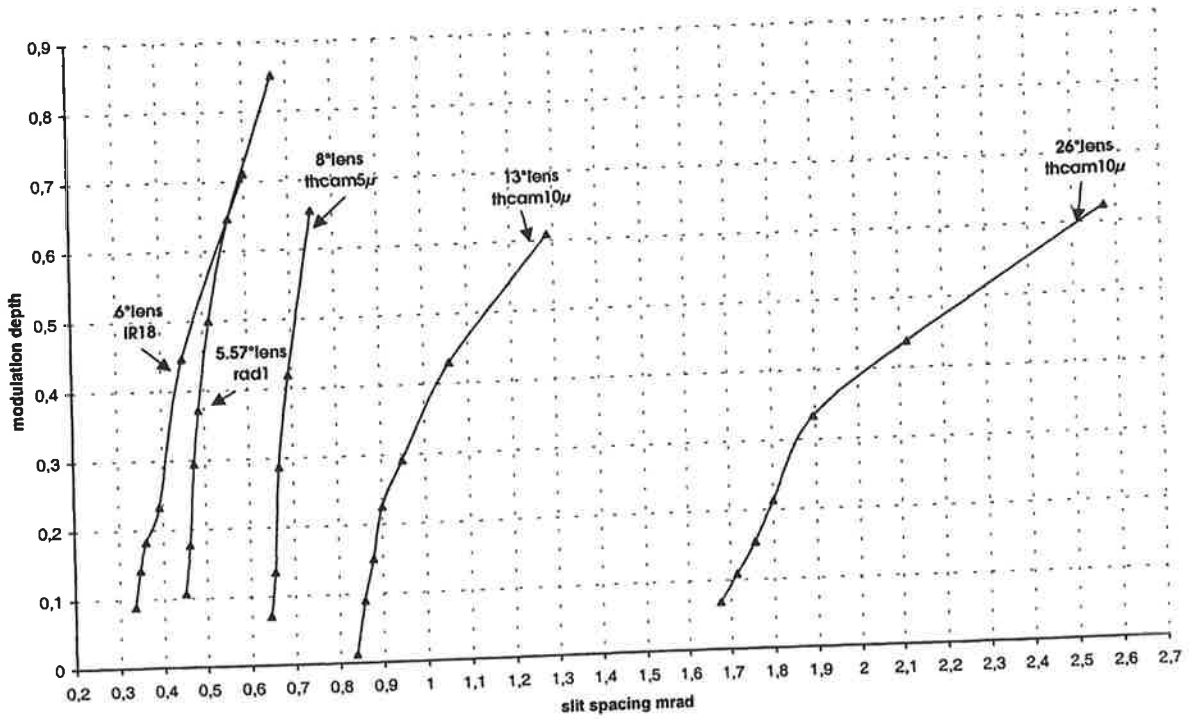

Figure 11: Modulation depth versus slit spacing for 5 different IR cameras.

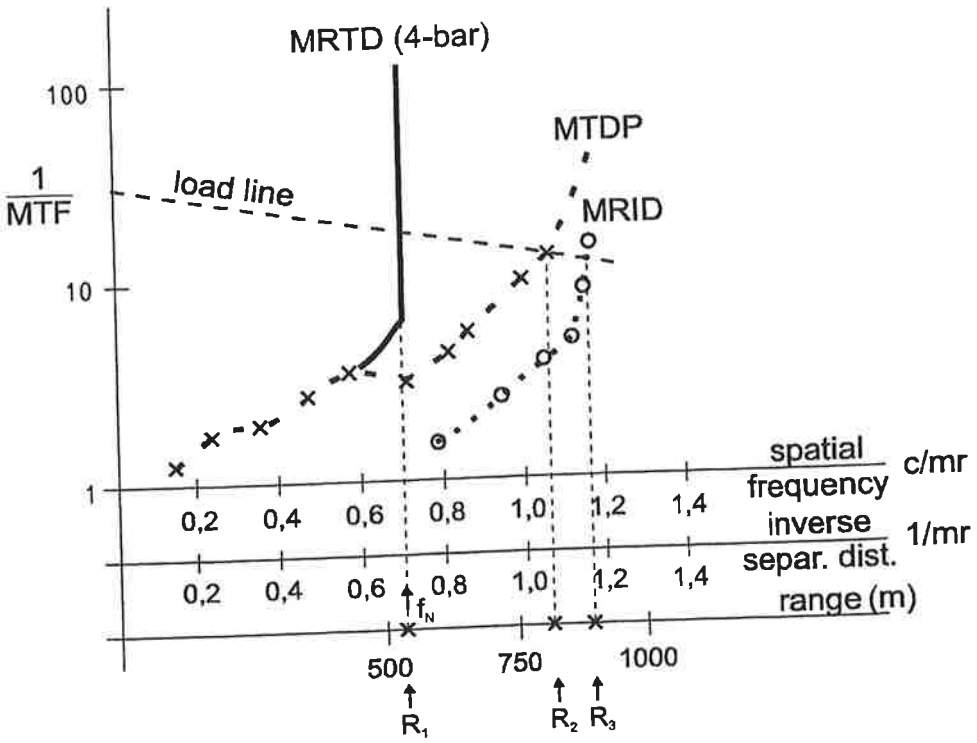

Figure 12: Comparison of range determination with MRTD, MTDP and MRID.

5. CONCLUSIONS

An alternative method has been described for the measurement of IR sensor performance. The method is based upon the use of two parallel line sources (double-slit), which has a number of advantages compared to the classical 4-bar patterns:

- no problems with aliasing effects, resulting in a wrong number of bars
- discrimination of the two lines is strongly depending on the separation distance, leading to a sensitive criterion
- the targets are easy to manufacture and cheap
- it is simple to vary the line distance and thus easy to measure the limiting geometrical resolution of a sensor
- the line sources are easy to model and handle in the frequency domain
- the method is suitable for objective as well as subjective performance measurements
- the method can simply be transferred into the STANAG4347 for range performance predictions.

Further validation in field experiments is recommended.

6. REFERENCES

[1] Wolfgang Wittenstein; Minimum Temperature Difference Perceived – A new approach to assess undersampled thermal imagers, Opt. Eng. Vol 38, No. 5, 1999

[2] Wolfgang Wittenstein, TRM3 progress report, Proceedings SPIE Vol 4130 (San Diego, August 2000), pp 292-302

[3] STANAG4349 LAND (Edition 1) – Measurement of the Minimum Resolvable Temperature Difference (MRTD) of Thermal Cameras, MAS/210-LAND/4349, August 1995

[4] Arie N. de Jong et al., Fast and objective Minimum Resolvable Temperature Difference measurement, Proc SPIE Vol 916 (London, June 1988)

[5] Arie N. de Jong, Description of an Infrared Zoom collimator, TNO report FEL-93-A034, March 1993

[6] Arie N. de Jong, Description of the LION Tester, TNO report FEL-01-A011, January 2001

[7] Max Born and Emil Wolf, Principles of Optics, Pergamon Press, 1964, pp 415-419

[8] Piet Bijl et al., TOD, the alternative to MRTD and MRC, Opt. Eng. Vol 37, No. 7, 1998

[9] Gerald C. Holst, Electro-Optical Imaging System Performance, SPIE-Press, 2nd edition, ISBN 0-8194-3701-8, 2000

[10] Ronald G. Driggers et al., Introduction to Infrared and Electro-Optical Systems, Artech House, Boston 1999, ISBN 0-89006-470-9

[11] Arie N. de Jong et al., The Nettuno trials of TG12, results of experiment B, July 1998, TNO report FEL-99-A189, April 2000

PROCEEDINGS OF SPIE
SPIE—The International Society for Optical Engineering

Infrared Imaging Systems: Design, Analysis, Modeling, and Testing XII

Gerald C. Holst
Chair/Editor

18–19 April 2001
Orlando, USA

Sponsored and Published by
SPIE—The International Society for Optical Engineering

Volume 4372